

Hall Effects On Heat and Mass Transfer Through a Porous Medium In a Rotating Channel With Radiation

Sudha Mathew¹, P. Raveendra Nath*¹ and N. B. V. Rama Deva Prasad²

¹*Department of Mathematics, Sri Krishnadevaraya University College of Engineering and Technology, S. K. University, Anantapur, A.P., India.*

²*Department of Mathematics, Balaji P. G. College, Anantapur, A.P., India*

ABSTRACT

we analyse the combined effects of Hall currents and radiation on the convective heat and mass transfer of a viscous electrically conducting fluid through a porous medium confined in a rotating horizontal channel in the presence of heat sources. The equations governing the flow, heat and mass transfer are solved exactly to obtain the velocity, temperature and concentration and are analysed for different variations of the governing parameters G, D^{-1}, M, m, N and α . The shear stress and the rate of heat and mass transfer are numerically evaluated for different sets of the parameters. The influence of the Hall currents and the radiation on the flow, heat and mass transfer characteristics are discussed in detail.

Keywords: Hall effect, CFD, Heat Transfer, Mass Transfer, Rotating channel, Radiation effect

INTRODUCTION

Free convection and mass transfer flow in porous medium has received considerable attention due to its numerous applications in geophysics and energy related problems. Such types of applications include natural circulation in isothermal reservoirs, aquifers, porous insulation in heat storage bed, grain storage extraction of thermal energy and thermal insulation design. Studies associated with flows through porous medium in rotating environment have some relevance in geophysical and geothermal applications. Many aspects of the motion in a rotating frame of reference of terrestrial and planetary atmosphere are influenced by the effects of rotation of the medium. Also buoyancy and rotational effects are often comparable in geophysical processes. Convective transport in a rotating atmosphere over a locally heated surface gives rise to dust storms (typhoons) and other atmosphere circulations.

The unsteady flow of a rotating viscous fluid in a channel maintained by non-tensional oscillations of one or both the boundaries has been studied by several authors to analyse the growth and development of boundary layers associated with geothermal flows for possible applications in geophysical fluid dynamics.[1]

Later Singh et al[2] studied free convection in MHD flow of a rotating viscous liquid in porous media. Singh et al [3] have also studied free convective MHD flow of a rotating viscous fluid in a porous medium past an infinite vertical porous plate.

Alam et al [4] have studied unsteady free convective heat and mass transfer flow in a rotating system with Hall currents, viscous dissipation and Joule heating.

Akiyama and chang [5] numerically analysed the influence of gray surface radiation on the convection of nonparticipating fluid in a rectangular enclosed space.

Recently, Ghaly [6], Chamkha et al.[7], Yussyo El-Dib and Ghaly[8], analyze the effect of radiation heat transfer on flow and thermal fields in the presence of a magnetic field for horizontal and inclined plates. Shohel Mahmud [9] studied the effects of radiation heat transfer on magneto hydrodynamic mixed convection through a vertical channel packed with fluid saturated porous substances.

AbdEl – Naby et al [10] studied the effects of radiation on unsteady free convective flow past a semi-infinite vertical plate with variable surface temperature using Crank – Nicolson finite difference method. Chamkha et al. [11] analyzed the effects of radiation on free convection flow past a semi-infinite vertical plate with mass transfer, by taking into account the buoyancy ratio parameter N Ganesan and Loganathan [12] studied the radiation and mass transfer effects flow of incompressible viscous fluid past a moving vertical cylinder using Rosseland approximation by the Crank – Nicolson finite difference method.

2. Formulation and solution of the problem

We consider the steady flow of an incompressible, viscous, electrically conducting fluid through a porous medium bounded by two parallel plates. In the undisturbed state, both the plates and fluid rotate with same angular velocity Ω and are maintained at constant temperature and concentration. Further the plates are cooled or heated by constant temperature gradient in some direction parallel to the plane of the plates. We choose a cartesian co-ordinate system $O(x,y,z)$ such that the plates are at $z=0$ and $z=L$ and the z -axis coincide with the axis of rotation of the plates. The steady hydromagnetic boundary layer equations of motion with respect to a rotating frame moving with angular velocity Ω under Boussinesq approximations are

$$-2\Omega v = -\frac{1}{\rho} \left(\frac{\partial p}{\partial x} \right) + \nu \left(\frac{\partial^2 u}{\partial z^2} \right) + (\mu_e H_0 J_y u) - \left(\frac{\nu}{k} \right) u \quad (2.1)$$

$$2\Omega u = -\frac{1}{\rho} \left(\frac{\partial p}{\partial y} \right) + \nu \left(\frac{\partial^2 v}{\partial z^2} \right) - (\mu_e H_0 J_x v) - \left(\frac{\nu}{k} \right) v \quad (2.2)$$

$$0 = -\frac{1}{\rho} \left(\frac{\partial p}{\partial z} \right) + \beta g (T - T_0) + \beta^* g (C - C_0) \quad (2.3)$$

The energy equation is

$$\rho_0 C_p \left(u \frac{\partial T}{\partial x} + v \frac{\partial T}{\partial y} \right) = k_1 \left(\frac{\partial^2 T}{\partial z^2} \right) + Q \quad (2.4)$$

The diffusion equation is

$$\left(u \frac{\partial C}{\partial x} + v \frac{\partial C}{\partial y} \right) = D_1 \left(\frac{\partial^2 C}{\partial z^2} \right) + k_{11} \left(\frac{\partial^2 T}{\partial z^2} \right) \quad (2.5)$$

where u, v are the velocity components along x and y directions respectively, p is the pressure including the centrifugal force, ρ is the density, k is the permeability constant, ν is the coefficient of kinematic viscosity, k_1 is the thermal diffusivity, D_1 is the chemical molecular diffusivity, β is the coefficient of thermal expansion, β^* is the volumetric coefficient of expansion with mass fraction, Q is the strength of the heat source and k_{11} is the cross diffusivity.

When the strength of the magnetic field is very large we include the Hall current so that the generalized Ohm's law is modified to

$$\bar{J} + \omega_e \tau_e (\bar{J} \times \bar{H}) = \sigma (\bar{E} + \mu_e (\bar{q} \times \bar{H})) \quad (2.6)$$

where \bar{q} is the velocity vector, \bar{H} is the magnetic field intensity vector, \bar{E} is the electric field, \bar{J} is the current density vector, ω_e is the cyclotron frequency, τ_e is the electron collision time, σ is the fluid conductivity and μ_e is the magnetic permeability.

Neglecting the electron pressure gradient, ion-slip and thermo-electric effects and assuming the electric field $\bar{E}=0$, equation (2.6) reduces to

$$J_x + mJ_y = \sigma\mu_e H_0 v \tag{2.7}$$

$$J_y - mJ_x = -(\sigma\mu_e H_0 u) \tag{2.8}$$

where $m = \omega_e \tau_e$ is the Hall parameter.

On solving equations (2.7) & (2.8) we obtain

$$J_x = \frac{\sigma\mu_e H_0}{1 + m^2} (v + mu) \tag{2.9}$$

$$J_y = \frac{\sigma\mu_e H_0}{1 + m^2} (mv - u) \tag{2.10}$$

Using the equations (2.9) & (2.10), the equations of motions governing the flow through a porous medium with respect to a rotating frame are given by

$$-2\Omega v = -\frac{1}{\rho} \left(\frac{\partial p}{\partial x} \right) + \nu \left(\frac{\partial^2 u}{\partial z^2} \right) + \left(\frac{\sigma\mu_e^2 H_0^2}{\rho_o (1 + m^2)} \right) (mv - u) - \left(\frac{\nu}{k} \right) u \tag{2.11}$$

$$2\Omega u = -\frac{1}{\rho} \left(\frac{\partial p}{\partial y} \right) + \nu \left(\frac{\partial^2 v}{\partial z^2} \right) - \left(\frac{\sigma\mu_e^2 H_0^2}{\rho_o (1 + m^2)} \right) (v + mu) - \left(\frac{\nu}{k} \right) v \tag{2.12}$$

$$0 = -\frac{1}{\rho} \left(\frac{\partial p}{\partial z} \right) + \beta g (T - T_0) + \beta^* g (C - C_0) \tag{2.13}$$

Combining (2.11) & (2.12) we get

$$-2i\Omega q = -\frac{1}{\rho_o} \left(\frac{\partial p}{\partial \xi} \right) - \left(\frac{\sigma\mu_e^2 H_0^2}{\rho_o (1 + m^2)} \right) (1 - im)q - \left(\frac{\nu}{k} \right) q + \nu \left(\frac{\partial^2 q}{\partial z^2} \right) \tag{2.14}$$

Where

$$q = u + iv$$

$$\xi = x - iy$$

$$\bar{\xi} = x + iy$$

Integrating (2.13) we get

$$\frac{P}{\rho_o} = \beta g \int (T - T_0) dz + \beta^* g \int (C - C_0) dz + \phi(\xi, \bar{\xi}) - gz \tag{2.15}$$

Using (2.15), equation(2.14) can be written as

$$-2i\Omega \bar{q} + \left(\frac{M^2 (1 - im)}{(1 + m^2)} \right) \bar{q} + \left(\frac{\nu}{k} \right) \bar{q} - \nu \left(\frac{\partial^2 \bar{q}}{\partial z^2} \right) = -2\beta g \left(\frac{\partial(T - T_0)}{\partial \xi} \right) - 2\beta^* g \left(\frac{\partial(C - C_0)}{\partial \xi} \right) \tag{2.16}$$

Since $\bar{q} = \bar{q}(z, t)$, equation (2.16) is valid if the temperature distribution and the concentration distribution are of the form

$$T - T_0 = \alpha_1 x + \beta_1 y + \theta_1(z, t)$$

$$C - C_0 = \alpha_2 x + \beta_2 y + C_1(z, t)$$

where α_1, β_1 are the gradients of temperature along O(x,y) respectively and α_2, β_2 are gradients of concentration along O(x,y), $\theta_1(z, t)$ is the arbitrary function of z and t.

We take

$$T_0 = \alpha_1 x + \beta_1 y + \theta_{1w}$$

$$T_0 = \alpha_1 x + \beta_1 y + \theta_{1w2}$$

to be the temperatures of the lower and upper plates respectively.

Similarly we take

$$C_0 = \alpha_2 x + \beta_1 y + C_{1w1}$$

$$C_0 = \alpha_2 x + \beta_2 y + C_{1w2}$$

to be the concentrations of the lower and upper plates respectively.

Using (2.14) and (2.15) and using (2.16) we get

$$-2i\Omega \bar{q} + \left(\frac{M^2(1-im)}{(1+m^2)} \right) \bar{q} + \left(\frac{\nu}{k} \right) \bar{q} - \nu \left(\frac{\partial^2 \bar{q}}{\partial z^2} \right) + \beta g \bar{A} z + (\beta^* g \bar{B} z) = D_2 \quad (2.17)$$

Where

$$D_2 = \frac{\partial \phi(\xi, \bar{\xi})}{\partial \xi}$$

$$A = \alpha_1 + \beta_1$$

$$B = \epsilon_2 + \beta_2$$

The non-dimensional variables are

$$z' = \frac{z}{L}, t' = \frac{t\nu}{L^2}, q' = \frac{q\nu}{L}, \omega' = \frac{\omega L^2}{\nu^2}, \theta' = \frac{\beta g L^3 (\theta_1 - \theta_{1w1})}{\nu^2}, C = \frac{\beta^* g L^3 (C_1 - C_{1w1})}{\nu^2}$$

The equations governing the flow, heat and mass transfer are (dropping the dashes)

$$\left(\frac{\partial^2 q}{\partial z^2} \right) - \lambda^2 q = G(1+N) - R \quad (2.18)$$

$$\left(\frac{\partial^2 \theta}{\partial z^2} \right) + \alpha = P(G_1 u + G_2 v) \quad (2.19)$$

$$\left(\frac{\partial^2 C}{\partial z^2} \right) + \left(\frac{ScSo}{N} \right) \left(\frac{\partial^2 \theta}{\partial z^2} \right) = Sc(G_{1c} u + G_{2c} v) \quad (2.20)$$

Where

$$\lambda^2 = \left(D^{-1} + 2iE^{-1} + \frac{M^2(1-im)}{1+m^2} \right)$$

$$E = \frac{\nu}{L^2 \Omega} \quad (\text{Ekman number})$$

$$D^{-1} = \frac{L^2}{k} \quad (\text{Darcy parameter})$$

$$(G_1, G_2) = \frac{\beta g L^4 (\alpha_1, \beta_1)}{\nu^2} \quad (\text{Grashof number})$$

$$(G_{1c}, G_{2c}) = \frac{\beta^* g L^4 (\alpha_2, \beta_2)}{\nu^2} \quad (\text{Modified Grashof number})$$

$$G = G_1 + iG_2, \quad G_c = G_{1c} + iG_{2c}$$

$$R = \frac{L^3 D_2}{\nu^2} \quad (\text{Reynolds number})$$

$$N = \frac{\beta^* \Delta C}{\beta \Delta T} \quad (\text{Buoyancy ratio})$$

$$P = \frac{\nu}{k} \quad (\text{Prandtl number})$$

$$\alpha = \frac{QL^2}{k_1} \quad (\text{Heat source parameter})$$

$$Sc = \frac{\nu}{D_1} \quad (\text{Schmidt number})$$

$$So = \frac{k_{11} \beta^*}{\beta \nu} \quad (\text{Soret number})$$

The boundary conditions are

$$q = 0 \quad \text{on } z = -1$$

$$q = 0 \quad \text{on } z = 1$$

$$\theta = 0, C = 0 \quad \text{on } z = -1$$

$$\theta = \frac{\beta g L^3 (\theta_{1w1} - \theta_{1w2})}{\nu^2} = \theta_0 \quad \text{on } z = 1 \tag{2.21}$$

$$C = \frac{\beta^* g L^3 (C_{1w1} - C_{1w2})}{\nu^2} = C_0 \quad \text{on } z = 1$$

Solving equations(2.18)-(2.20) subject to the boundary conditions(2.21) we obtain

$$q = \frac{R}{\lambda^2} \left(\frac{\text{Cosh}(\lambda z)}{\text{Cosh}(\lambda)} - 1 \right) + \frac{G}{\lambda^2} \left(\frac{\text{Sinh}(\lambda z)}{\text{Sinh}(\lambda)} - z \right)$$

$$\theta = GP \text{ Re al} \left(\frac{A_1}{\lambda^2} \text{Cosh}(\lambda z) - \cosh(\lambda) \right) + \frac{A_2}{\lambda^2} (\text{Sinh}(\lambda z) - z \text{Sinh}(\lambda))$$

$$- \frac{G}{6\lambda^2} (z^3 - z) - \frac{R}{\lambda^2} (z^2 - 1) + \alpha_1 (z^2 - 1) + \frac{\theta_0}{2} (1 - z)$$

$$C = A_5 \text{ Re al} \left(\frac{A_1}{\lambda^2} \text{Cosh}(\lambda z) - \cosh(\lambda) \right) + \frac{A_2}{\lambda^2} (\text{Sinh}(\lambda z) - z \text{Sinh}(\lambda))$$

$$- \frac{G}{6\lambda^2} (z^3 - z) - \frac{R}{\lambda^2} (z^2 - 1) - \frac{A_6}{2} (z^2 - 1)$$

3. Flow Rate ,Shear Stress,Nusselt Number And Sherwood Number

The non-dimensional flow rate is given by

$$Q = (Q_x + iQ_y) = \int_{-1}^1 q dz \tag{3.1}$$

$$= \frac{2}{\lambda^2} (A_1 \text{Sinh}(\lambda) + R)$$

Shear stress on the walls $z = \pm 1$ are given by

$$\begin{aligned}\tau &= (\tau_x + i\tau_y)_{z=\pm 1} = \left(\frac{dq}{dz} \right)_{z=\pm 1} \\ &= \lambda (\pm A_1 \text{Sinh}(\lambda) + A_2 \text{Cosh}(\lambda)) - \left(\frac{G}{\lambda^2} \right)\end{aligned}\quad (3.2)$$

Local rate of heat transfer across the walls (Nusselt number) is given by

$$\begin{aligned}(Nu)_{z=\pm 1} &= \left(\frac{d\theta}{dz} \right)_{z=\pm 1} \\ &= GP \text{Re} al \left(\left(\frac{(\pm A_1 \text{Sinh}(\lambda) + A_2 \text{Cosh}(\lambda))}{\lambda} - \frac{G}{\lambda^2} \mp \frac{R}{\lambda^2} \right) \pm \alpha_1 + A_3 \right)\end{aligned}\quad (3.3)$$

Rate of mass transfer (Sherwood number) is given by

$$\begin{aligned}(Sh)_{z=\pm 1} &= \left(\frac{dC}{dz} \right)_{z=\pm 1} \\ &= A_5 \text{Re} al \left(\left(\frac{(\pm A_1 \text{Sinh}(\lambda) + A_2 \text{Cosh}(\lambda))}{\lambda} - \frac{G}{\lambda^2} \mp \frac{R}{\lambda^2} \right) \pm A_6 + A_7 \right)\end{aligned}\quad (3.4)$$

where

$$A_1 = \frac{R}{\lambda^2 \text{Cosh}(\lambda)}$$

$$A_2 = \frac{G}{\lambda^2 \text{Sinh}(\lambda)}$$

$$A_3 = GP \text{Re} al \left(\frac{G}{6\lambda^2} - \frac{A_2}{\lambda^2} \text{Sinh}(\lambda) - \frac{R}{2\lambda^2} \right)$$

$$A_4 = -0.5\alpha_1 + 0.5\theta - GPR + \left(\frac{A_1 \text{Cosh}(\lambda)}{\lambda^2} - \frac{R}{2\lambda^2} \right)$$

$$A_5 = GN \text{Sc} - \left(\frac{\text{ScSo}GP}{N} \right)$$

$$A_6 = \frac{\text{ScSo}\alpha_1}{N}$$

$$A_7 = A_5 \text{Re} al \left(\frac{G}{6\lambda^2} - \frac{A_2}{\lambda^2} \text{Sinh}(\lambda) \right) + \frac{C_0}{2}$$

$$A_8 = A_{55} \text{Re} al \left(-\frac{R}{\lambda^2} + \frac{A_1}{\lambda^2} \text{Cosh}(\lambda) \right) + \frac{C_0}{2} + \frac{A_6}{2}$$

DISCUSSION OF THE NUMERICAL RESULTS

The velocity and temperature profiles are drawn for different positive and negative G. It is to be noted that in all the profiles drawn we have taken G to be real so that the applied pressure gradient in OX-direction is positive or negative according as the walls are heated or cooled in the axial direction (i.e G>0 or G<0).

From Fig.1 we notice that an increase in the rotation parameter k reduces |u|. When the molecular buoyancy forces dominates over the thermal buoyancy force, |u| enhances when the buoyancy forces act in the same direction while it reduces when they are in opposite directions.

The effect of Hall Currents on u is exhibited in Fig.2. We find that u experiences an enhancement with increase in the Hall parameter m with maximum at z=0.6. Also the reversal flow zone enhances marginally with m.

The transverse velocity v is exhibited in Figs.3 and 4 for different variations of G , k , N and m . From Fig.3 we find that lesser the permeability of the porous medium or higher the Lorentz force, smaller the magnitude of v everywhere in the flow region. The effect of rotation of the fluid on v exhibits an increasing tendency with rotation parameter k . When the molecular buoyancy force dominates over the thermal buoyancy force, the secondary velocity enhances when the forces act in the same direction and depreciates when they act in opposite directions. Fig.4 shows that the magnitude of v enhances with increase in the Hall parameter m with maximum at $z=0.6$.

The temperature distribution θ is shown in Figs.5-7 for different values of N , k , m and α . The temperature is positive or negative according as the actual temperature is greater or less than the equilibrium temperature.

An increase in the rotation parameter k depreciates the temperature. When the molecular buoyancy force dominates over the thermal buoyancy force the temperature enhances in the lower half and reduces in the upper half when they act in same direction while for the forces acting in opposite directions the actual temperature reduces in the lower half and enhances in the upper half of the channel Fig.5.

Fig.6 shows that An increase in the Hall parameter m enhances the actual temperature in the entire flow region.

The behaviour of θ with the heat source parameter α shows that an increase in α depreciates in the lower half and enhances in the upper half while an increase in $\alpha > 0$ enhances the actual temperature Fig.7.

The shear stress τ at the walls $z = 0$ and $z = 1$ have been evaluated for different values of G , M , N , m , D^{-1} and k are presented in Tables.1- 4. The component of stress in the x -direction is positive in the heating case and negative in the cooling case An increase in G enhances the components of τ at both the walls. The variation of τ_x with D^{-1} and M shows that lesser the permeability or higher the Lorentz force, smaller the magnitude of stress components (Tables.1 and 2).

The behavior of the stress components with the rotation parameter k reveals that τ_x experiences a reduction at the walls When the molecular buoyancy force dominates over the thermal buoyancy force, the stress components enhance in magnitude when the buoyancy forces are in the same direction while for the forces acting in opposite directions they experience a depreciation (Tables 3 and 4). An increase in the Hall parameter m leads to an enhancement in the magnitude of the stress components.

The average Nusselt Number (Nu) which measures the rate of heat transfer at the walls $z = 0$ and $z = 1$ has been exhibited in (Tables. 5-10) for different parametric values. It is found that Nu at $z = 0$ and $z = 1$ is negative in both heating and cooling cases. The rate of heat transfer at both the walls enhances with increase in $|G|$. An increase in D^{-1} and M depreciates Nu (Tables 5 and 6). An increase in k depreciate Nu at both the walls. Also Nu decreases with increase in $N > 0$ and enhances with $|N| < 0$ (Tables. 7 and 8).

An increase in $\alpha > 0$ enhances Nu at $z=0$ and reduces it at $z = 1$. Also a reversed effect is noticed in the case of a heat sink (Tables. 9 and 10).

The Sherwood number (Sh) which measures the rate of mass transfer is presented in (Tables. 11-14) for different G , D^{-1} , M , m , k and N . We find that the Sherwood number enhances with G at both the walls. Also lesser the permeability of the porous medium or higher the Lorentz force, smaller the magnitude of Sh at $z = 0$ and $z = 1$ (Tables. 11 and 12).

An increase in the rotation parameter k depreciates Sh at both the walls. When the molecular buoyancy force dominates over the thermal buoyancy force, the magnitude of Sh increases when the forces act in the same direction and reduces when they act in opposite directions. (Tables. 13 and 14)

Table.1 Shear Stress (τ_x) at $z = 0$ $P=0.71, k=0.5, N=1$

G/τ	I	II	III	IV	V	VI	VII
10^3	4.6063	3.3238	2.7368	4.3921	3.7964	4.6275	4.6347
3×10^3	9.3116	6.7179	5.5312	8.8784	7.6736	9.3546	9.3690
-10^3	-4.8043	-3.4645	-2.8519	-4.5804	-3.9580	-4.8265	-4.8339
-3×10^3	-9.5096	-6.8587	-5.6463	-9.0667	-7.8351	-9.5535	-9.5683

Table.2 Shear Stress(τ_x) at z=1

G/ τ	I	II	III	IV	V	VI	VII
10^3	4.8043	3.4645	2.8519	4.5804	3.9579	4.8265	4.8339
3×10^3	9.5096	6.8587	5.6463	9.0667	7.8351	9.5535	9.5683
-10^3	-4.6063	-3.3238	-2.7368	-4.3921	-3.7964	-4.6275	-4.6347
-3×10^3	-9.3116	-6.7180	-5.5312	-8.8780	-7.6736	-9.3546	-9.3689

	I	II	III	IV	V	VI	VII
D^{-1}	5×10^2	10^3	3×10^3	5×10^2	5×10^2	5×10^2	5×10^2
M	2	2	2	5	10	2	2
m	0.5	0.5	0.5	0.5	0.5	1.5	2.5

Table.3 Stress(τ_x) at z=0

G/ τ	I	II	III	IV	V	VI
10^3	4.6063	4.6021	4.5794	7.0815	0.8935	0.6025
3×10^3	9.3116	9.3030	9.2571	14.2619	1.8861	0.9906
-10^3	-4.8043	-4.7999	-4.7761	-7.2795	-1.0915	-1.0125
-3×10^3	-9.5096	-9.5008	-9.4539	-14.4599	-2.0841	-1.9616

Table.4 Stress(τ_x) at z=1

G/ τ	I	II	III	IV	V	VI
10^3	4.8043	4.7999	4.7761	7.2795	1.0916	0.9986
3×10^3	9.5096	9.5008	9.4539	14.4599	2.0841	1.9802
-10^3	-4.6063	-4.6021	-4.5794	-7.0815	-0.8935	-0.8246
-3×10^3	-9.3116	-9.3030	-9.2571	-14.2619	-1.8861	-1.8012

	I	II	III	IV	V	VI
K	0.5	1.5	2.5	0.5	0.5	0.5
N	1	1	1	2	-0.5	-0.8

Table.5 Nusselt Number(Nu) at z = 0 P=0.71,k=0.5,N=1

G/ Nu	I	II	III	IV	V	VI	VII
10^3	-1.4541	-1.0379	-0.8849	-1.3771	-1.1759	-1.4618	-1.4644
3×10^3	-4.2655	-2.5601	-1.9337	-3.9494	-3.1248	-4.2971	-4.3078
-10^3	-1.5396	-1.0825	-0.9152	-1.4547	-1.2337	-1.5481	-1.5511
-3×10^3	-4.4365	-2.6492	-1.9941	-4.1048	-3.2403	-4.4697	-4.4809

Table.6 Nu at z=1

G/ Nu	I	II	III	IV	V	VI	VII
10^3	-0.4487	0.0084	0.1757	-0.3638	-0.1427	-0.4572	-0.4603
3×10^3	-3.3455	-1.5583	-0.9032	-3.0138	-2.1494	-3.3788	-3.3899
-10^3	-0.3632	0.0529	0.2061	-0.2861	-0.0849	-0.3709	-0.3735
-3×10^3	-3.1745	-1.4692	-0.8428	-2.8585	-2.0342	-3.2062	-3.2169

	I	II	III	IV	V	VI	VII
D^{-1}	5×10^2	10^3	3×10^3	5×10^2	5×10^2	5×10^2	5×10^2
M	2	2	2	5	10	2	2
m	0.5	0.5	0.5	0.5	0.5	1.5	2.5

Table.7 Nu at z=0

G/ Nu	I	II	III	IV	V	VI
10^3	-1.4541	-1.4522	-1.4421	-1.3366	-1.6302	-1.5812
3×10^3	-4.2655	-4.2577	-4.2159	-3.7957	-4.9702	-4.2721
-10^3	-1.5396	-1.5375	-1.5262	-1.4222	-1.7157	-1.4137
-3×10^3	-4.4365	-4.4282	-4.3843	-3.9667	-5.1411	-4.8727

Table.8 Nu at z=1

G/ Nu	I	II	III	IV	V	VI
10^3	-0.4487	-0.4466	-0.4353	-0.3312	-0.6248	-0.6642
3×10^3	-3.3455	-3.3373	-3.2934	-2.8758	-4.0502	-4.2542
-10^3	-0.3632	-0.3613	-0.3511	-0.2457	-0.5393	-0.5895
-3×10^3	-3.1745	-3.1667	-3.1251	-2.7048	-3.8791	-4.1278

	I	II	III	IV	V	VI
K	0.5	1.5	2.5	0.5	0.5	0.5
N	1	1	1	2	-0.5	-0.8

Table.9 Nu at z = 0 P=0.71,k=0.5,N=1

G/ Nu	I	II	III	IV	V	VI
10 ³	-1.4541	-1.9995	-2.5449	-0.3632	0.1823	0.7277
3x10 ³	-4.2655	-4.8109	-5.3564	-3.1745	-2.6291	-2.0836
-10 ³	-1.5396	-2.0851	-2.6305	-0.4487	0.0968	0.6422
-3x10 ³	-4.4365	-4.9819	-5.5274	-3.3456	-2.8001	-2.2544

Table.10 Nu at z=1

G/ Nu	I	II	III	IV	V	VI
10 ³	-0.4487	0.0968	0.6422	-1.5396	-2.0850	-2.6305
3x10 ³	-3.3455	-2.8001	-2.2544	-4.4365	-4.9819	-5.5274
-10 ³	-0.3632	0.1823	0.7277	-1.4541	-1.9995	-2.5451
-3x10 ³	-3.1745	-2.6291	-2.0836	-4.2655	-4.8109	-5.3564

	I	II	III	IV	V	VI
α	2	4	6	-2	-4	-6

Table.11 Sherwood Number(Sh) at z = 0 P=0.71,k=0.5,N=1

G/Sh	I	II	III	IV	V	VI	VII
10 ³	1.1713	0.6305	0.4306	1.0724	0.8112	1.1812	1.1845
3x10 ³	4.6851	2.5221	1.7223	4.2895	3.2447	4.7246	4.7378
-10 ³	1.1712	0.6305	0.4305	1.0722	0.7994	1.1811	1.1768
-3x10 ³	4.6849	2.5221	1.7221	4.2890	3.2432	4.7244	4.6896

Table.12 Sherwood Number(Sh) at z=1

G/Sh	I	II	III	IV	V	VI	VII
10 ³	-5.5029	-2.9751	-2.0516	-5.0321	-3.8088	-5.5502	-5.5661
3x10 ³	-21.4377	-11.6014	-8.0034	-19.6088	-14.8476	-21.6215	-21.683
-10 ³	-4.9299	-2.6761	-1.8487	-4.5106	-3.4212	-4.9709	-4.9849
-3x10 ³	-20.2897	-11.0032	-7.5977	-18.5634	-14.0723	-20.4628	-20.5211

	I	II	III	IV	V	VI	VII
D ⁻¹	5x10 ²	10 ³	3x10 ³	5x10 ²	5x10 ²	5x10 ²	5x10 ²
M	2	2	2	5	10	2	2
m	0.5	0.5	0.5	0.5	0.5	1.5	2.5

Table.13 Sherwood Number(Sh) at z=0

G/Sh	I	II	III	IV	V	VI
10 ³	1.1713	1.1689	1.1566	2.1864	-0.6442	-0.5402
3x10 ³	4.6852	4.6757	4.6263	8.7457	-2.5766	-2.3782
-10 ³	1.1712	1.1686	1.1565	2.1863	-0.66441	-0.5812
-3x10 ³	4.6849	4.6589	4.6260	8.7455	-2.5766	-2.2782

Table.14 Sherwood Number(Sh) at z=1

G/Sh	I	II	III	IV	V	VI
10 ³	-5.5029	-5.4911	-5.4278	-9.5852	3.2842	2.8545
3x10 ³	-21.4377	-21.3918	-21.1461	-37.1926	12.8499	11.1467
-10 ³	-4.9289	-4.9185	-4.8626	-8.4371	2.9972	2.6446
-3x10 ³	-20.2897	-20.2465	-20.0156	-34.8965	12.2759	10.1047

	I	II	III	IV	V	VI
K	0.5	1.5	2.5	0.5	0.5	0.5
N	1	1	1	2	-0.5	-0.8

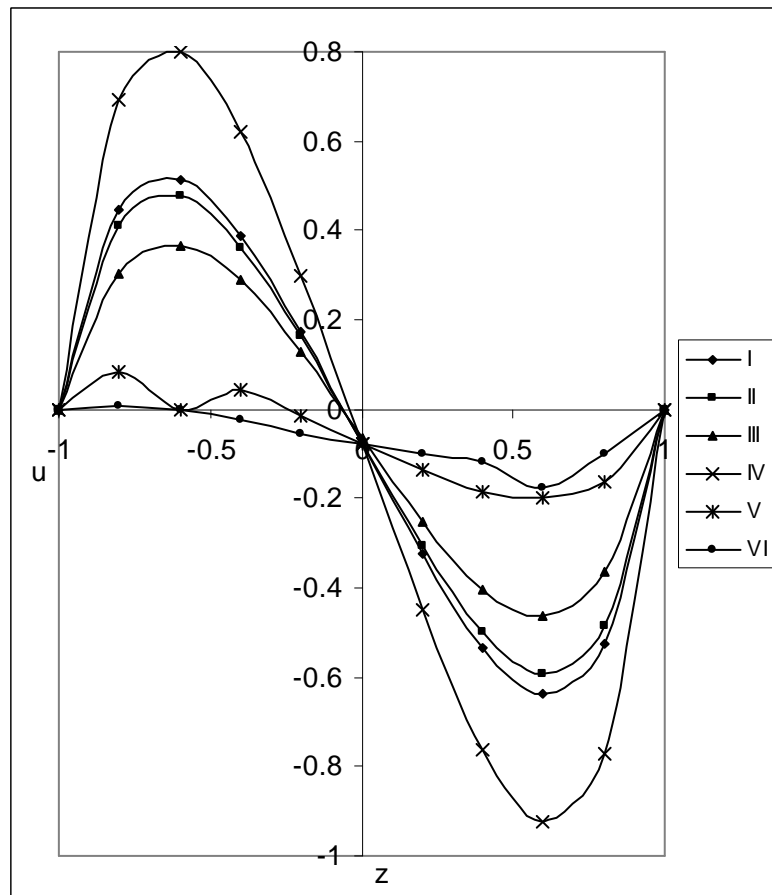


Fig.1 u with K&N,G=10³,M=2,m=0.5

	I	II	III	IV	V	VI
K	0.5	1.0	1.5	0.5	0.5	0.5
N	1	1	1	2	-0.5	-0.8

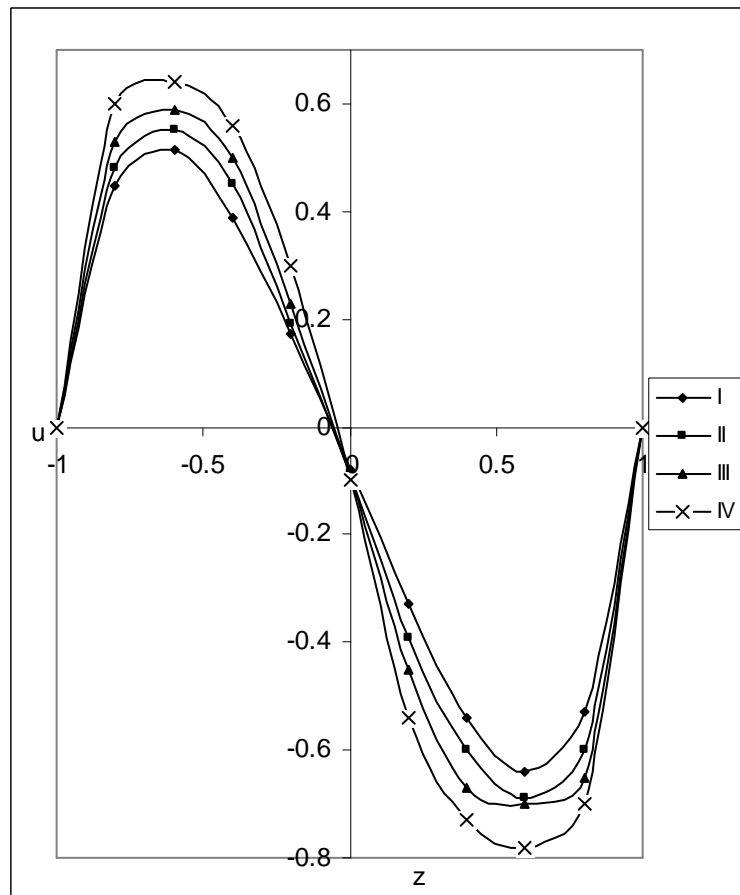


Fig.2 u with $m=10^3, N=1, k=0.5$

	I	II	III	IV
m	0.5	1.0	1.5	2.0

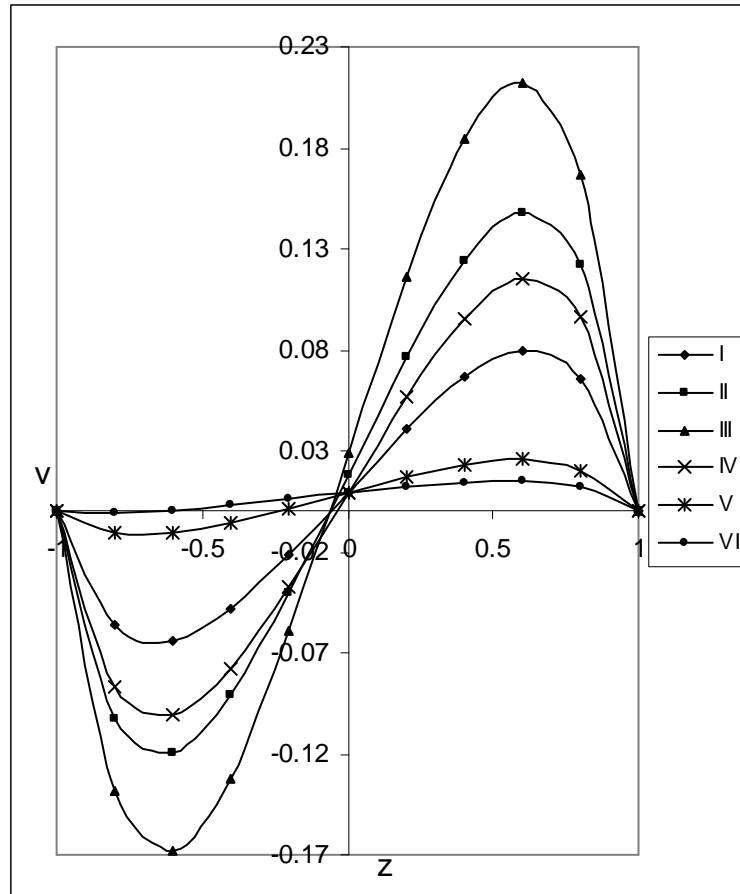


Fig.3 v with K&N, $G=10^3, M=2, m=0.5$

	I	II	III	IV	V	VI
K	0.5	1.0	1.5	0.5	0.5	0.5
N	1	1	1	2	-0.5	-0.8

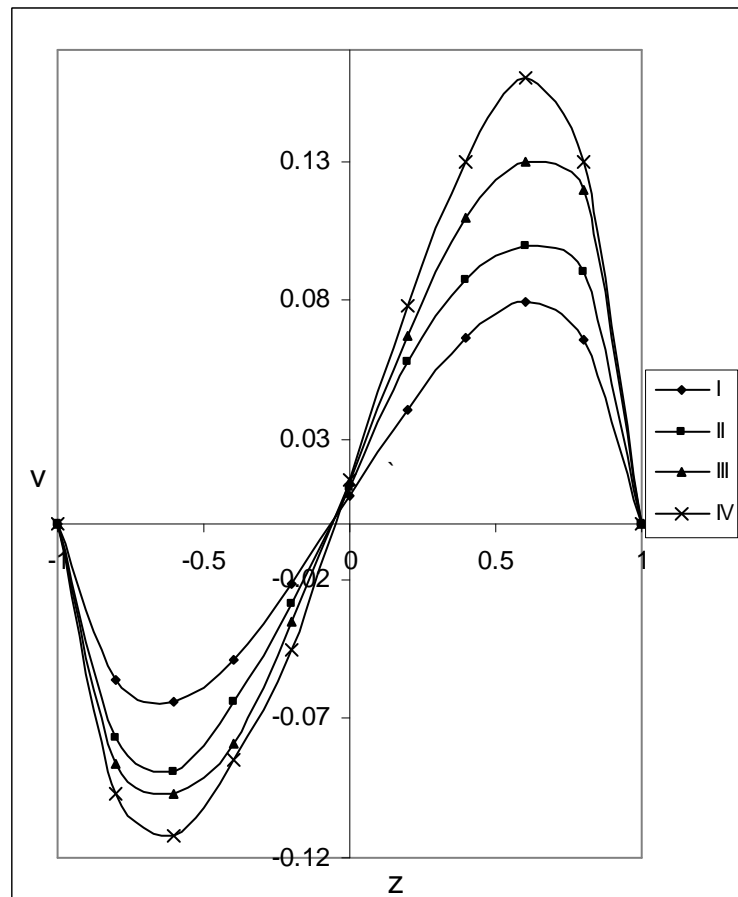


Fig.4 v with $m G=10^3, N=1, k=0.5$

	I	II	III	IV
m	0.5	1.0	1.5	2.0

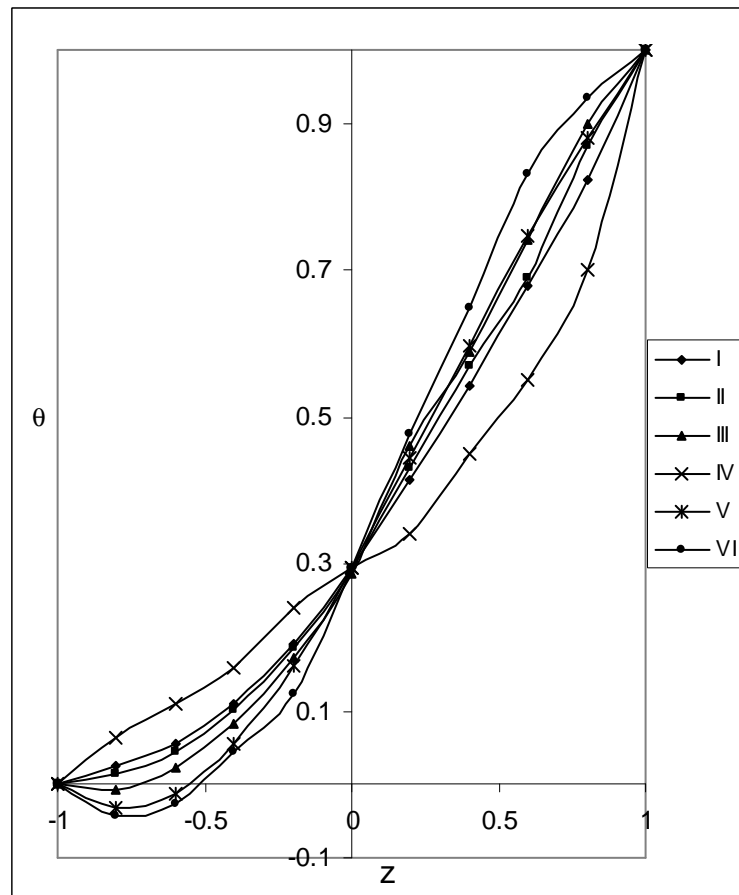


Fig.5 θ with K&N $G=10^3, M=2, m=0.5$

	I	II	III	IV	V	VI
K	0.5	1.0	1.5	0.5	0.5	0.5
N	1	1	1	2	-0.5	-0.8

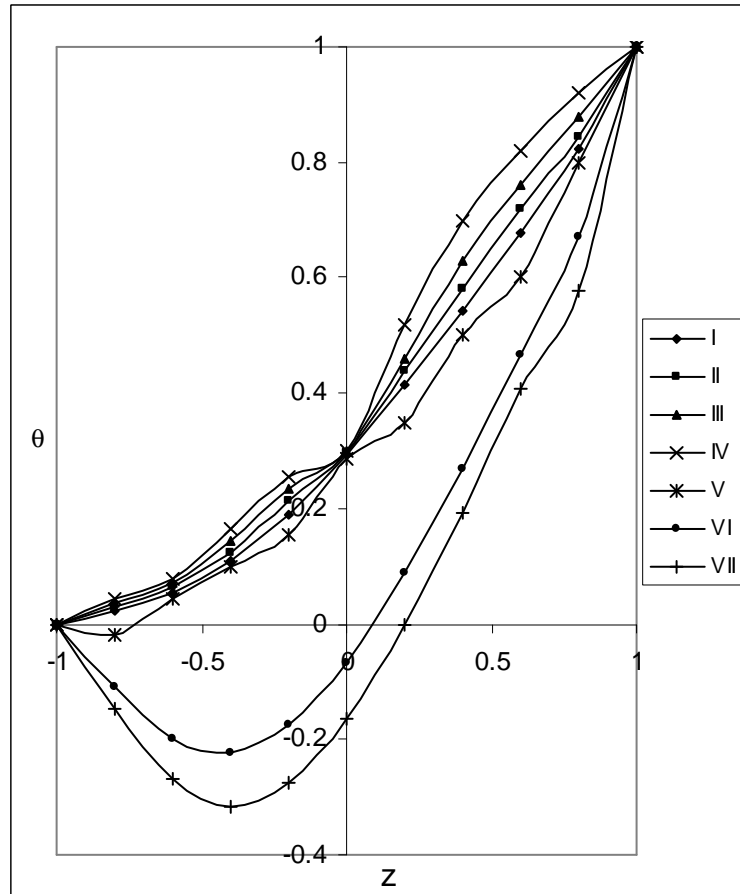


Fig.6 θ with $m = 10^3, N=1, k=0.5$

	I	II	III	IV	V	VI	VII
m	0.5	1.0	1.5	2.0	0.5	0.5	0.5
N1	0.5	0.5	0.5	0.5	1.0	4.0	10.0

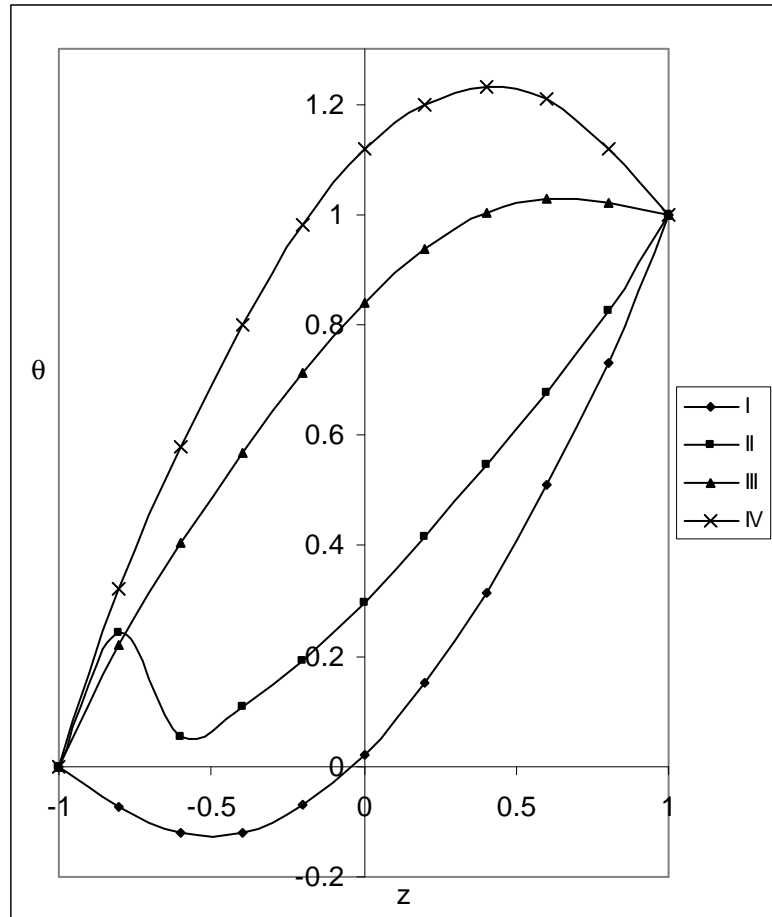


Fig.7 θ with α

I	II	III	IV
α	2	4	-2 -4

REFERENCES

[1] Krishna, D.V., Prasadarao D.R.V., Ramachandra Murty A.S., J. Engg. Physics and Thermo. Physics, 75(2002)281-291.
 [2] Singh N.P, Gupta S.K., and Singh, Atul Kumar, : Proc. Nat. Acad. Sci, India, 71(2001)149-157.
 [3] Singh N.P, Ajay Kumar, Yadav M.K., and Singh Atul Kumar, : Ind. Theor. Phy. 50(2002) 37-43.
 [4] Alam M.M and Sattar M.A., : Journal of Energy heat and mass transfer, 22 (2000)31-39.
 [5] Akiyama M, and Chong, : Numerical Heat Transfer Part A , 32 (1997) 419-33.
 [6] Ghaly A.Y., : Chaos Solitons and Fractals , 13 (2002)13:1843-1850.
 [7] Chamkha A.J., Issa, C, Khanfer, K., : Int. J .Thermal Sci. 41(2002)73-81.
 [8] Yussyo El-Dib, AY., Ghaly, : Chaos Solitons and Fractals, 18, Issue 1, (2003) 55-68.
 [9] Shohel Mahmud, Roydon Andrew Fraser, : Journal of Energy 28 (2003) 1557-1577.
 [10] Abd El – Naby M.A., Elsayed M.E., : Journal of Applied mathematics, 2, (2003) 65-86.
 [11] Chamkha A.J., Takhar H.S., and Soundalgekar V.M., : Journal of chemical Engineering 84, (2001) 335-342.
 [12] Ganesan P, and Logantham P, : International Journal of Heat and Mass Transfer , 45 (2002) 4281-4288.